Crystal chemistry of the G-phases in the systems Ti–{Fe, Co, Ni}–Al with a novel filled variant of the Th 6Mn 23-type

Article *in* Intermetallics · April 2003

DOI: 10.1016/S0966-9795(02)00267-4

CITATIONS
28

READS
1,038

11 authors, including:

Andriy Grytsiv
University of Vienna
230 PUBLICATIONS **5,068** CITATIONS
SEE PROFILE

Peter Franz Rogl
University of Vienna
910 PUBLICATIONS **16,616** CITATIONS
SEE PROFILE

Francois Weill
Institut de Chimie de la matière condensée de Bordeaux
180 PUBLICATIONS **5,972** CITATIONS
SEE PROFILE

Henri Noël
Université de Rennes 1
421 PUBLICATIONS **6,163** CITATIONS
SEE PROFILE

Available online at www.sciencedirect.com
SCIENCE DIRECT®
Intermetallics 11 (2003) 351–359
Intermetallics
www.elsevier.com/locate/intermet

Crystal chemistry of the G-phases in the systems Ti–{Fe, Co, Ni}–Al with a novel filled variant of the Th_6Mn_{23}-type

Andriy Grytsiv[a], Jin Jun Ding[a], Peter Rogl[a,*], François Weill[b], Bernard Chevalier[b], Jean Etourneau[b], Gilles André[c], Françoise Bourée[c], Henri Noël[d], Peter Hundegger[e], Günter Wiesinger[e]

[a]*Institut für Physikalische Chemie, Universität Wien, A-1090 Wien, Währingerstr. 42, Austria*
[b]*Institut de Chimie de la Matiére Condensée de Bordeaux (ICMCB) CNRS-UPR 9048, Université de Bordeaux I, Ave. Dr. A. Schweitzer, 33608 Pessac, Cedex, France*
[c]*Laboratoire Léon Brillouin (CEA-CNRS), CEA/Saclay, F-91191 Gif-sur-Yvette, France*
[d]*Laboratoire de Chimie du Solide et Inorganique Moléculaire, Université de Rennes I, UMR CNRS-6511, Avenue du Général Leclerc, F-35042 Rennes cedex, France*
[e]*Institut für Festkörperphysik, TU Wien, A-1040 Wien, Wiedner Hauptstr. 8-10, Austria*

Received 25 October 2002; accepted 12 December 2002

Abstract

The crystal structures of the compounds $Ti_6M_7Al_{17}$ with M = Fe,Co,Ni have been investigated by X-ray powder and single crystal, neutron powder and electron diffraction. These compounds crystallize with a new filled variant of the $Mg_6Cu_{16}Si_7$-type (space group $Fm\bar{3}m$). A close structural relation is encountered for the series of crystal structures: $Th_6Mn_{16}Mn_7$?, $Mg_6Cu_{16}Si_7$?, $Sc_6Sc_{16}Ir_7Ir$, $Zr_6Zn_{16}Zn_7Si$, $Ti_6Al_{16}M_7Al$, and $Ti_6Ni_{16}Si_7Si$. Electrical resistivity of the Fe, Co-based compounds is typical metallic and temperature dependence follows the Bloch Grüneisen relation with a Debye temperature of about 300 K. No hydrogen was found to be absorbed in the Fe-, and Co-based compounds at room temperature under a H_2 pressure of 5 MPa.

Keywords: A. Titanium aluminides; B. Crystallography; B. Electrical resistance; B. Hydrogen storage; F. Diffraction (electron, neutron and X-ray)

1. Introduction

From recent investigations of the phase relations in the ternary systems Ti–M–Al, M being a metal from the 8th group, we encountered a series of isotypic ternary solution phases [1–4], which from their cubic symmetry and unit cell dimensions seemed to correspond to the so-called G-phases [5]. Numerous literature data [6] reveal for these compounds an approximate formula $TiMAl_{\sim 2}$ and preliminarily assigned the Th_6Mn_{23}- or $Mg_6Cu_{16}Si_7$-type. Although scandium compounds $Sc_6M_7Al_{16}$, M = Co,Ni,Ru,Rh,Pd,Os,Ir, are known to adopt the ordered $Mg_6Cu_{16}Si_7$-type [8], Rietveld refinements of X-ray powder intensity data for corresponding Ti-compounds with platinum metals and $TiCoAl_{\sim 2}$, however, indicated a filling of the octahedral void in the 4b-site[1] by a metal atom [3,4]. Cage filling in the structure type of Th_6Mn_{23} has been observed for a variety of intermetallic compounds such as in $Sc_{11}Ir_4$ [9] and $Zr_6Zn_{23}Si$ [10]. It should be mentioned here, that hydrogen and deuterium atoms in the rare earth (RE) containing phases, $RE_6M_{23}\{H,D\}_x$ (as high as $x = 23$ in $Y_6Mn_{23}D_x$ [11]), preferentially occupy the 4b-sites of the Th_6Mn_{23}-structure [12].

Although the homogeneity regions of the G-phases and their structures have been monitored by Rietveld analyses [3,4], neither atomic positions nor atom distribution in the crystal structure of the Ti–M–Al G-phases (M = Fe,Co,Ni) are known with high precision. In view of the various structure types closely related of $Mg_6Cu_{16}Si_7$ [13], all deriving from the parent Th_6Mn_{23}-type, new

* Corresponding author. Tel.: +43-1-4277-52456; fax: +43-1-4277-95245.
E-mail address: peter.franz.rogl@univie.ac.at (P. Rogl).

[1] Originally assumed 4a-site but after standardization of crystal structure [7] is assigned as 4b-site of $Fm\bar{3}m$.

0966-9795/03/$ - see front matter © 2003 Elsevier Science Ltd. All rights reserved.
PII: S0966-9795(02)00267-4

variations of the Th_6Mn_{23}-type are conceivable. Therefore, in this paper we present a detailed evaluation of the crystal structures of the G-phases in ternary systems Ti–{Fe,Co,Ni}–Al, employing X-ray single crystal- and neutron powder diffraction as well as electron diffraction (SAED). Additionally, the crystal structures of the corresponding compounds in the ternary systems Ti–Si–Ni and Hf–Ni–Al were re-inspected in order to get a general view on the crystal chemistry of the G-phases. Finally, the potential to absorb hydrogen gas in the Ti–M–Al G-phases (M = Fe,Co,Ni) was investigated, particularly in view of a perspective use of G-phases as creep resistance enhancing precipitates (age hardening) in TiAl-based duplex alloys.

2. Experimental details

Samples were prepared by argon arc-melting on a water-cooled cooper hearth in Ti-gettered argon from elemental ingots with minimal purity of 99.9 wt.%. X-ray powder diffraction data were collected from a D5000 or from a Guinier-Huber image plate system with Cu-$K_{\alpha 1}$ radiation. Neutron powder diffraction was carried out at room temperature on the spectrometer 3T2 of the ORPHEE 14 MW-reactor of CEA/Saclay with $\lambda_{neutron} = 0.122510$ nm and resolution $\Delta d/d \geqslant 4\times10^{-3}$. A 10 g sample $Ti_{23}Ni_{24}Al_{53}$ annealed at 900 °C was prepared for the neutron diffraction investigation. Prior to crushing the sample to a 25 μm grain size powder, single crystal specimens were selected for X-ray single crystal investigation. Quantitative Rietveld refinements of the X-ray and neutron data were performed with the FULLPROF program [14].

Single crystals were mechanically isolated from crushed as-cast alloys with nominal compositions $Ti_{23}Fe_{26}Al_{51}$, $Ti_{30}Co_{25}Al_{45}$ and $Ti_{23}Ni_{24}Al_{53}$. From each alloy two single crystal specimens of similar dimensions were investigated. Weissenberg photographs accomplished crystal quality control prior to X-ray intensity data collection on a four circle Nonius Kappa diffractometer equipped with a CCD area detector employing graphite monochromated MoK_α radiation ($\lambda = 0.071073$ nm). Orientation matrix and unit cell parameters for a cubic system were derived using the program DENZO [15]; absorption corrections were made by program SORTAV [15], approximating the irregular crystal shape by crystal planes. The structures were refined with the aid of the SHELXS-97 program [16]. Electron diffraction (SAED) was performed at 200 keV on a Jeol 2000 FX microscope. Prior to the observation, the alloys were crushed in alcohol and a drop of the suspension was deposited on a copper grid with lacey carbon.

The electrical resistivity was measured from the surface of polished samples using a four probe d.c.-method in the temperature range from 4.2 to 200 K. Hydrogen absorption was studied at room temperature in an high pressure balance system under 5 MPa H_2 for alloys $Ti_{23}Ni_{24}Al_{53}$, $Ti_{23}Fe_{26}Al_{51}$, $Ti_{30}Co_{25}Al_{45}$, $Ti_{44}Fe_{26}Al_{30}$ and $Ti_{47}Co_{28}Al_{25}$. An amount of 1000 mg was put into the sample holder of a Satorius-high-pressure-balance performing at an accurcy of 10 μg. Each sample was activated by heating at 200 °C in a vacuum of 2×10^{-6} mbar for 24 h. Subsequently hydrogen was introduced with a pressure of 5 MPa and the sample allowed to cool down to ambient temperature. The mass of the sample was monitored during the whole loading procedure.

3. Results and discussion

3.1. Single crystal structure determination of as-cast compounds

Single crystal intensity data from samples $Ti_{23}Fe_{26}Al_{51}$, $Ti_{30}Co_{25}Al_{45}$ and $Ti_{23}Ni_{24}Al_{53}$ confirmed in all cases cubic symmetry (space group $Fm\bar{3}m$) with a unit cell of about 1.2 nm. CCD-frames and TEM-exposures (Fig. 1) did not reveal any supercell formation. Structure solution by direct methods with program SIR prompted an atom arrangement in general correspondence with the Th_6Mn_{23}-type as reported earlier [17]. Refinement of this structure model converged to low residual values for a distribution of atoms similar to that reported for the $Mg_6Cu_{16}Si_7$-type. However, in contrast to the Th_6Mn_{23}-structure an additional Al atom is clearly revealed in the 4b site (1/2,1/2,1/2) from difference Fourier plots for all crystals investigated (Tables 1–3). Occupancies and thermal displacement parameters were refined independently for all atom sites and indicated rather complete atom order for the Fe- and Ni-containing crystal specimens. Slightly higher temperature factures for the 4b-site (about two times the displacement parameter of atoms in the 4a site) indicated partial occupation of about 80% Al in the Ti-poor specimens. Significant random distribution of atoms was found for the cobalt-based compound where titanium and aluminum atoms share the three crystallographic sites 4b, 24e and 32f (Table 1). These findings agree well with the X-ray powder data of [4] on the wide homogeneity region of the G-phase in the Ti–Co–Al system, which extends at 950 °C within the atomic ratio $0.3 < Al/(Ti + Al) < 0.7$ at cobalt contents slightly varying from 25 to 28 at.% Co.

Similarly to the Ti–Co–Al system, a wide homogeneity region was reported for the Ti–Fe–Al G phase at 800 and 900 °C [18,19]. According to [18] the Ti–Fe–Al G-phase was found in a cubic modification at high titanium contents and a tetragonal modification at high aluminum contents. The tetragonal modification could

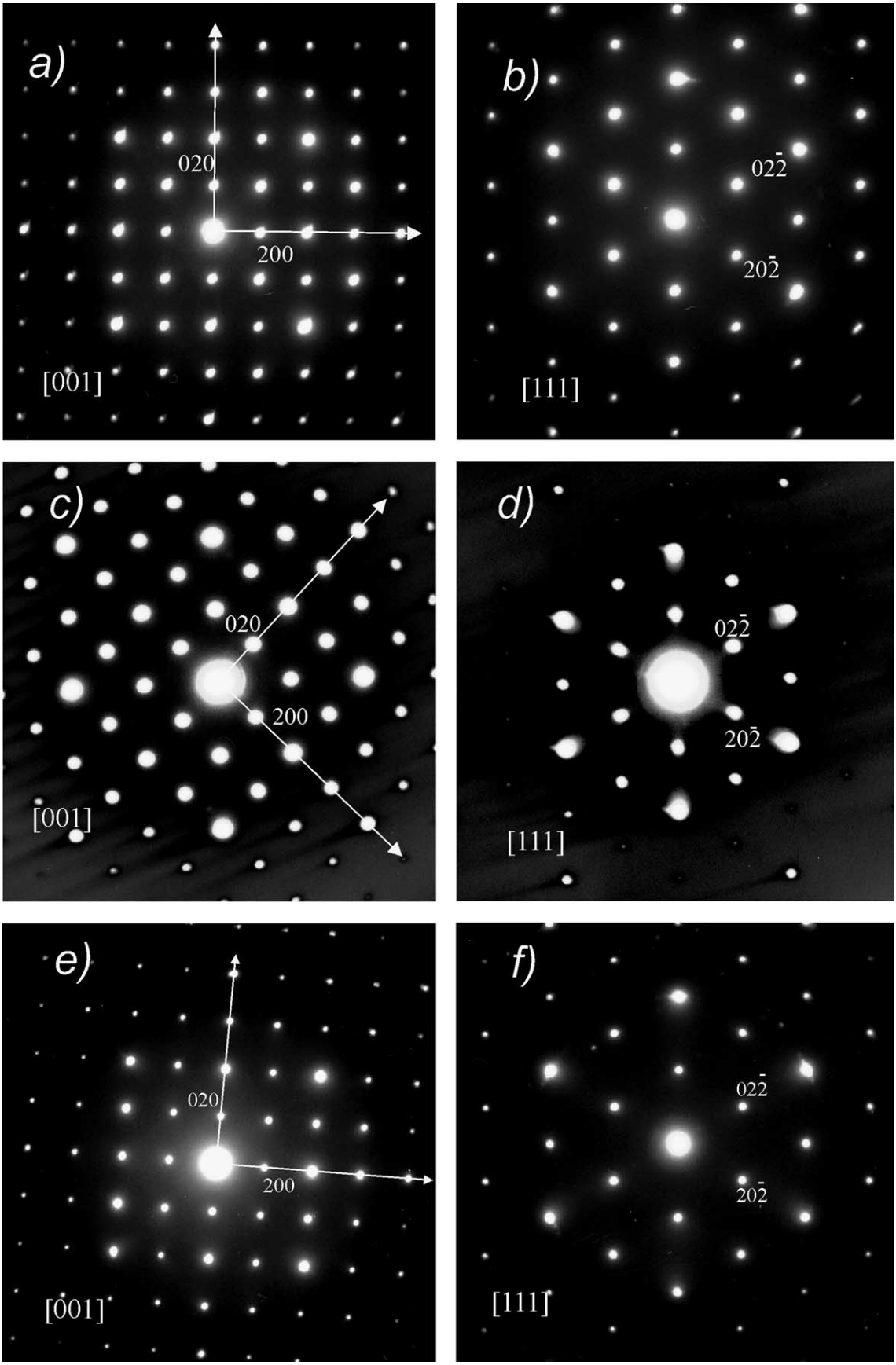

Fig. 1. Electron diffraction patterns of G-phases in the ternary systems Ti–Fe–Al (*a,b*), Ti–Co–Al (*c,d*) and Ti–Ni–Al (*e, f*).

be reliably observed only in two-phase samples, and appeared associated with weak additional reflections. At a temperature of 1000 °C the two modifications were separated by an immiscibility gap [18,20], and it was suggested in a recent review by [21], that both modifications have an individual field of primary crystallization. With

Table 1
Single crystal data for $Ti_6Al_7M_{17}$ {M = Fe,Co,Ni} (filled Th_6Mn_{23}-type, space group $Fm\bar{3}m$; No. 225; origin at centre)

Parameter/alloy composition		$Ti_{23}Fe_{26}Al_{51}$	$Ti_{30}Co_{25}Al_{45}$	$Ti_{23}Ni_{24}Al_{53}$
Formula from refinement (at.%)		$Ti_{20.3}Fe_{23.7}Al_{56.0}$	$Ti_{27.5}Co_{23.4}Al_{49.1}$	$Ti_{23.1}Ni_{23.5}Al_{53.4}$
Crystal size		60×84×72 μm³	56×42×56 μm³	70×84×92 μm³
a (nm)		1.18898(4)	1.19356(3)	1.18933(4)
Data collection, 2Θ range (°)		2⩽2Θ⩽62; 200 s/frame	2⩽2Θ⩽60; 300 s/frame	2⩽2Θ⩽70; 180 s/frame
Total number of frames		148	164	154
Reflections in refinement (total)		150⩾4σ(Fo) of 175 [4192]	148⩾4σ(Fo) of 163 [4619]	202⩾4σ(Fo) of 232 [4525]
mosaicity (absorption coeff. mm^{-1})		<0.43 [8.64]	<0.36 [10.82]	<0.45 [11.86]
Number of variables		19	22	19
$R_F^2 = \Sigma\lvert F_0^2\text{-}F_c^2\rvert/\Sigma F_0^2$		0.0430	0.0283	0.0413
R_{Int}		0.0127	0.071	0.074
GOF		1.114	1.095	
Extinction (Zachariasen)		0.0003(1)	0.0009(2)	0.0004(1)
Atom parameters				
M1 in 4a (0,0,0); occ.		1.00(1)Fe	1.00(1) Co	1.00(1) Ni
$U_{11} = U_{22} = U_{33}$		0.0086(8)	0.0085(6)	0.0113(6)
M2 in 4b (1/21/21/2); occ.		0.81(3)Al	0.570(4)Ti + 0.430Al	0.82(4) Al
$U_{11} = U_{22} = U_{33}$		0.014(2)	0.0107(9)	0.010(2)
M3 in 24d (0, 1, 1/4, 1/4); occ.		1.00(1)Fe	1.00(1) Co	1.00(1) Ni
U_{11}; $U_{22} = U_{33}$; U_{23}		0.0046(8); 0.0064(6); 0.0008(5)	0.0085(6); 0.010(5); 0.0008(4)	0.0066(5); 0.0093(4); −0.0011(4)
M4 in 24e (x,0,0); x		0.2906(3)	0.2902(1)	0.2905(2)
occ.		1.00(1)Ti	0.866(4)Ti + 0.134 Al	Ti
U_{11}; $U_{22} = U_{33}$		0.040(2); 0.0104(9)	0.0154(9); 0.0089(5)	0.0353(13); 0.0092(5)
M5 in 32f (x,x,x); x		0.3412(2)	0.3417(1)	0.3410(1)
occ.		1.00(1)Al	1.00(1) Al	1.00(1) Al
$U_{11} = U_{22} = U_{33}$; $U_{12} = U_{13} = U_{23}$		0.0118(8); 0.0020(7)	0.0114(6); 0.0018(4)	0.0100(5); 0.0017(5)
M6 in 32f (x,x,x); x		0.1202(1)	0.12014(8)	0.1203(1)
occ.		1.00(1)Al	0.312(4)Ti + 0.688 Al	0.111(4)Ti + 0.889 Al
$U_{11} = U_{22} = U_{33}$; $U_{12} = U_{13} = U_{23}$		0.0090(7); 0.0003(6)	0.0085(5); −0.00015(31)	0.0096(5); 0.0006(4)
Residual density; max; min in (electrons/ nm^3)×1000		2.05;−3.12	1.20; −0.87	4.18; −3.25
Interatomic distances (nm), standard deviations are less than 0.0005 nm				
M1	8M6	0.2475	0.2484	0.2478
	6M4	0.3454	0.3464	0.3455
M2	6M4	0.2491	0.2504	0.2492
	8M5	0.3268	0.3272	0.3275
M3	4M5	0.2433	0.2442	0.2433
	4M6	0.2609	0.2619	0.2609
	4M4	0.3011	0.3022	0.3012
M4	1M2	0.2491	0.2504	0.2492
	4M5	0.2736	0.2742	0.2741
	4M6	0.2861	0.2869	0.2862
	4M3	0.3011	0.3022	0.3012
M5	3M3	0.2433	0.2442	0.2433
	3M6	0.2707	0.2722	0.2704
	3M4	0.2736	0.2742	0.2741
	3M5	0.3070	0.3096	0.3061
	1M2	0.3268	0.3272	0.3275
M6	1M1	0.2475	0.2484	0.2478
	3M3	0.2609	0.2619	0.2609
	3M5	0.2707	0.2722	0.2704
	3M6	0.2858	0.2868	0.2861
	3M4	0.2861	0.2869	0.2862

Table 2
Architecture of crystal structures derived from Th_6Mn_{23}-type

Compound	Th_6Mn_{23}	$Mg_6Cu_{16}Si_7$	$Sc_{22}Ir_8$	$Zr_6Zn_{23}Si$	$Ti_6Al_{17}Fe_7$	$Ti_6Ni_{16}Si_8$
Reference	[26]	[13]	[9]	[10]	This work	This work
Type	*Unfilled*	*Unfilled*	*Filled*	*Filled*	*Filled*	*Filled*
a (nm)	1.2523	1.165	1.3350	1.28384(1)	1.18898(4)	1.12532(3)
M1, 4*a*(0,0,0)	Mn	Si	Ir	0.9Zn	Fe	0.9Si + 0.1Ni
M2, 4*b*(1/2,1/2,1/2)	–	–	Ir	Si	0.8 Al	0.87Si
M3, 24*d*(0,1/4,1/4)	Mn	Si	Ir	Zn	Fe	Si
M4, 24*e*(*x*,0,0),	Th	Mg	Sc	Zr	Ti	Ti
x	0.297	0.3176	0.3005(8)	0.28959(7)	0.2906(3)	0.28767(8)
M5, 32*f*(*x*,*x*,*x*),	Mn	Cu	Sc	Zn	Al	Ni
x	0.322	0.3316	0.3433(3)	0.33563(4)	0.3412(1)	0.33388(3)
M6, 32*f*(*x*,*x*,*x*),	Mn	Cu	Sc	Zn	Al	Ni
x	0.122	0.1230	0.1167(4)	0.12277(4)	0.1202(2)	0.11864(4)

respect to these data, we performed a detailed inspection of X-ray powder diffraction patterns from aluminum-rich single phase samples (G-phase) in as-cast condition as well as after annealing at 800 and 900 °C: no tetragonal distortion was observed in bulk materials as well as in single crystals selected from as-cast samples. It is thus likely that the tetragonal phase is metastable, only forming on quenching from high temperatures, as suggested earlier by [22].

Following the suggestion [21] of a primary crystallization field for the titanium-rich G-phase, we attempted to obtain single crystals from titanium rich as-cast samples. However, the as-cast alloy $Ti_{47}Fe_{27}Al_{26}$, which lies inside the primary crystallization region of [21], does not contain any G-phase but TiFe- and $TiFe_2$-based phases. After annealing the G-phase appears. The X-ray powder diffraction Rietveld refinement for the sample $Ti_{43}Fe_{24}Al_{33}$, annealed at 900 °C for 10 days, presented in Table 3, clearly reveals filling of the 4b site, as generally observed in the aluminum-rich G-phase of the Ti–{Fe,Co,Ni}–Al systems (see Table 1). The random distribution of Ti- and Al-atoms corresponds to that observed for the Ti–Co–Al G-phase.

3.2. Neutron powder and X-ray single crystal diffraction of $Ti_{23}Ni_{24}Al_{53}$, annealed at 900 °C

With respect to the rather close X-ray scattering factors of the elements forming the G-phases in the Ti–{Fe,Co,Ni}–Al systems, and to counteract a misinterpretation of atom distribution, where the electron density from Ti-atoms can be simply accounted as a sum of Al and M-atoms, neutron diffraction was employed particularly because of the strong difference in the nuclear scattering factors of Ti (negative scattering length) and that of Al and Ni atoms. The results of the refinement of neutron powder intensities for $Ti_{22.5}Ni_{24.5}Al_{53}$ are summarized in Table 3 and unambiguously locate only Ti-atoms in the 24e site. Furthermore, practically full atom order in this compound is confirmed. Thermal displacement parameters if Ti-atoms in 24e, obtained from the X-ray single crystal refinement, however, revealed an elongated elliptical atom shape suggesting a split atom position with 79% of Ti at $x = 0.2861$ and 21% Ti at $x = 0.3205$ forming a larger and a smaller cage around the 4b site (Table 3). Employing this model for the neutron data simultaneously resulted in a significant improvement of reliability factors. As seen from the results of the X-ray refinement for the Fe- and Co-containing crystals selected from as-cast alloys, temperature displacement parameters of Ti atoms in 24e appear systematically nonsymmetrical (Table 1). Although the effect is by far smaller than for the annealed specimen of $Ti_6Al_7Ni_{17}$, a split position is indicated. Neutron and X-ray data are in fine agreement: small differences may be due to the fact that the neutron diffraction experiment averages over about 1 cm^3 polycrystalline sample volume, whilst the single crystal covers only a limited number of unit cells of a single grain.

3.3. Rietveld refinements for $Hf_6Al_{16}Ni_7$ and $Ti_6Ni_{16}Si_8$

The new data on the crystal chemistry of the G-phases in the Ti–{Fe,Co,Ni}–Al systems prompted us to expand our investigations on related ternary compounds particularly to $Hf_6Al_{16}Ni_7$, for which the $Mg_6Cu_{16}Si_7$-type [5] was derived from a "semi-quantitative" structure determination and to the Ti–Ni–Si G-phase [23,24]. In a recent experimental reinvestigation of the Ti–Ni–Si system [25] the Th_6Mn_{23} prototype was assigned.

Rietveld refinement of the X-ray powder data collected from $Hf_6Al_{16}Ni_7$ confirmed the atom distribution earlier reported for this phase by Ganglberger et al. [5]. A similar refinement for an as-cast alloy $Ti_{19}Ni_{57}Si_{24}$, however, reveals a filled structure as derived for the G-phases in Ti–{Fe,Co,Ni}–Al systems. The main difference is that the 4b site is occupied by Si-atoms, which are allocated also in 4a and 24d sites (chemical formula $Ti_6Ni_{16}Si_7Si$), whilst in $Ti_6Al_{16}M_7Al$ {M = Fe,Co,Ni}

Table 3
Crystal structure of $Ti_6Al_7Ni_{17}$ and $Ti_{13}Fe_7Al_{10}$ (filled Th_6Mn_{23}-type, Space Group $Fm\bar{3}m$; No. 225; origin at centre)

Parameter/alloy composition		$Ti_{22.5}Ni_{24.5}Al_{53}$[a]	$Ti_{22.5}Ni_{24.5}Al_{53}$[a]	$Ti_{43}Fe_{24}Al_{33}$
Heat treatment		900 °C	900 °C	900 °C
Refined composition in at.%		$Ti_{20.2}Ni_{23.5}Al_{56.3}$	$Ti_{20.1}Ni_{23.5}Al_{56.4}$	$Ti_{42}Fe_{23.3}Al_{34.7}$
a (nm)		1.19071(2)	1.18920(3)	1.20915(3)
Data collection		Neutron diffraction	Nonius Kappa/CCD	D5000
Radiation		$\lambda = 0.12272$ nm	MoK_α	Cu$K_{\alpha_{1,2}}$
Reflections measured (total)		175	$244 \geqslant 4\sigma$(Fo) of 320 (4156)	186
Θ range		$8 \leqslant 2\Theta \leqslant 124$	$2 \leqslant 2\Theta \leqslant 70$; 180 s/frame, 144 frames	$15 \leqslant 2\Theta \leqslant 110$
Number of variables		20	21	27
$R_F = \Sigma\|F_0 - F_c\|/\Sigma F_0$		0.057	$R_{Int} = 0.068$	0.066
$R_I = \Sigma\|I_{0B} - I_{cB}\|/\Sigma I_{0B}$		0.066	$R_F^2 = \Sigma\|F_0^2 - F_c^2\|/\Sigma F_0^2 = 0.0419$	0.070
$R_{wP} = [\Sigma w_i\|y_{0i} - y_{ci}\|^2/\Sigma w_i\|y_{0i}\|^2]^{1/2}$		0.075	Crystal size $90\times84\times112$ μm^3	0.087
$R_P = \Sigma\|y_{0i} - y_{ci}\|/\Sigma\|y_{0i}\|$		0.056	mosaicity < 0.45; abs.coeff 11.86 mm^{-1}	0.069
$R_e = [(N-P+C)/(\Sigma w_i y_{0I}^2)]^{1/2}$		0.032	Extinction (Zachariasen) = 0.0006(2)	0.045
$\chi^2 = (R_{wP}/R_e)^2$		5.58	GOF = 1.094	3.63
Atom parameters				
M1 in 4*a* (0, 0, 0), occ.		1.0(1)Ni	1.00(1) Ni	1.0(1)Fe
B_{eq} (B_{iso}) 10^2(nm^3)		0.39(4)	$U_{eq} = 0.0122(4)$[b]	0.4(1)
M2 in 4*b* (1/2, 1/2, 1/2), occ.		0.76(3) Al	0.80(2)Al	0.74Al + 0.26(2)Ti
B_{eq} (B_{iso}) 10^2(nm^3)		0.7(2)	Ueq = 0.010(1)[b]	0.9(2)
M3 in 24*d* (0,1/4,1/4), occ.		1.0(2)Ni	1.00(1) Ni	1Fe
B_{eq} (B_{iso}) 10^2(nm^3)		0.36(2)	Ueq = 0.0098(3)[b]	0.78(6)
M4 in 24*e* (*x*,0,0), *x*		0.2829(3) [0.3195(8)]	0.2861(2) [0.3205 (9)]	0.2861(2)
		0.62(1)Ti [0.38(1)Ti]	0.789(4)Ti [0.211(4)Ti]	1Ti
B_{eq} (B_{iso}) 10^2(nm^3), occ.		0.18(8)	Ueq = 0.0116(4)[0.011(1)][b]	0.92(7)
M5 in 32*f* (*x*, *x*, *x*), *x*		0.3412(2)	0.34064(7)	0.3411(1)
occ.		1.0(3)Al	1.00(1) Al	0.67Al + 0.33(3)Ti
B_{eq} (B_{iso}) 10^2(nm^3)		0.28(4)	Ueq = 0.0116(4)[b]	0.9(1)
M6 in 32*f* (*x*, *x*, *x*), *x*		0.1205(2)	0.12000 (7)	0.1204(1)
occ.		1.0(3) Al	1.00(1)Al	0.53Al + 0.47(3)Ti
B_{eq} (B_{iso}) 10^2(nm^3)		0.65(3)	Ueq = 0.0084(3)[b]	0.96(6)
Interatomic distances (nm), standard deviations are less than 0.0005 nm				
M1	8M6	0.2485	0.2472	0.2522
	6M4	0.3368[0.3806]	0.3402[0.3811]	0.3459
M2	6M4	0.2585[0.2148)	0.2544[0.2135]	0.2586
	8M5	0.3275	0.3282	0.3328
M3	4M5	0.2436	0.2432	0.2473
	4M6	0.2610	0.2611	0.2652
	4M4	0.3002[0.3090]	0.3004[0.3090]	0.3054
M4	1M2	0.2585[0.2148]	0.2544[0.2134]	0.2686
	4M5	0.2763[0.2686]	0.2757[0.2691]	0.2797
	4M6	0.2803[0.3120]	0.2824[0.3124]	0.2873
	4M3	0.3002[0.3090]	0.3004[0.3090]	0.3054
M5	3M3	0.2436	0.2432	0.2473
	3M6	0.2706	0.2706	0.2749
	3M4	0.2761[0.2686]	0.2757[0.2691]	0.2797
	3M5	0.3071	0.3049	0.3116
	1M2	0.3275	0.3282	0.3329
M6	1M1	0.2485	0.2472	0.2522
	3M3	0.2610	0.2611	0.2652
	3M5	0.2706	0.2706	0.2749
	3M6	0.2870	0.2854	0.2912
	3M4	0.2803[0.3120]	0.2824[0.3124]	0.2873

[a] Values in square brackets correspond to second (split) position of M4.

[b] M1(Ni): $U_{11} = U_{22} = U_{33} = 0.0122(4)$; M2(Al): $U_{11} = U_{22} = U_{33} = 0.010(1)$; M3(Ni): $U_{11} = 0.0081(4)$, $U_{22} = U_{33} = 0.0106(3)$; $U_{23} = -0.0013(2)$; M4(Ti): $U_{11} = 0.0125(11)$[0.0149(39)], $U_{22} = U_{33} = 0.0111(6)$[0.0091(19)]; M5(Al): $U_{11} = U_{22} = U_{33} = 0.0116(4)$, $U_{12} = U_{13} = U_{23} = 0.0028(4)$; M6(Al): $U_{11} = U_{22} = U_{33} = 0.0084(4)$, $U_{12} = U_{13} = U_{23} = 0.0007(3)$.

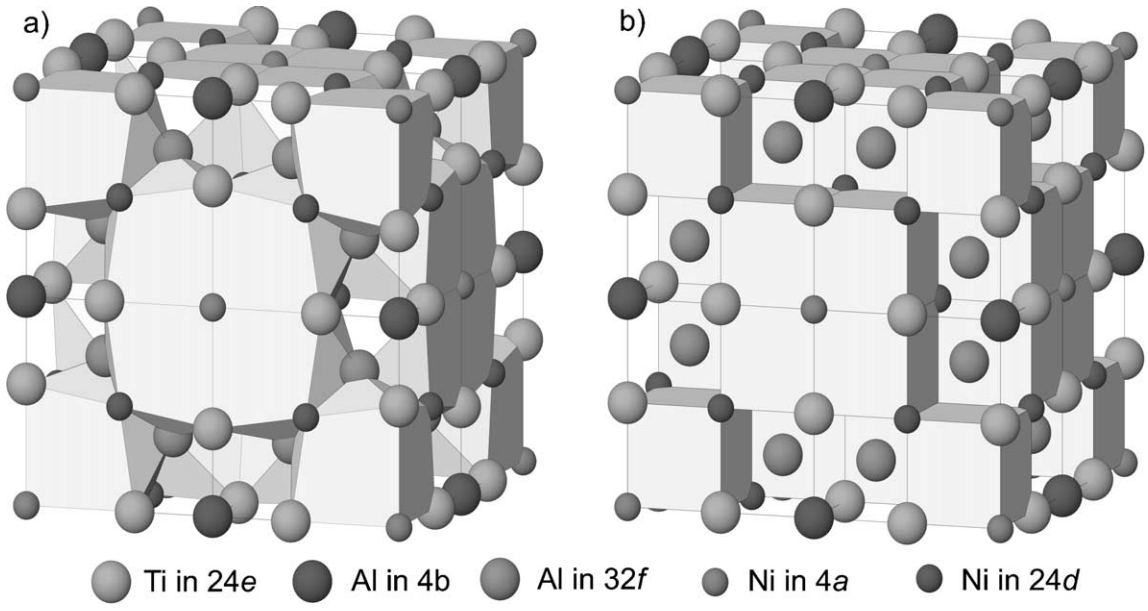

Fig. 2. Crystal structure of $Ti_6Al_7Ni_{17}$, (a) presented with coordination polyhedra around aluminum atoms (M6) in 32f site; (b) idealized model. Note the void in 8c (1/4,1/4,1/4).

the 4b site is occupied by Al atoms, which are located also in the two 32f sites. Therefore, $Ti_6Ni_{16}Si_8$ and $Ti_6Al_7M_{17}$ are two different filled variants of the $Mg_6Cu_{16}Si_7$-type, which in fact are closely related to the $Sc_{11}Ir_4$ structure type (see Table 2).

3.4. Crystal chemistry of G-phases

Among the numerous descriptions of Th_6Mn_{23} derivative structures, the analysis of Chabot et al. [9] is rather complete; it focuses on individual coordination polyhedra as well as on large clusters similar to those found in γ-brass or $Li_{22}Si_5$. Here we intend to cast a different view on these structures. A three-dimensional representation of the $Ti_6Al_7Ni_{17}$ structure is presented in Fig. 2a, emphasizing on the polyhedra around M6 atoms. The structure can thus be decomposed into 64 polyhedra of two types surrounding the atoms M5 and M6 in the 32f sites. It is interesting to note, that these polyhedra are based on distorted body-centered cubic "subcells". A simple transformation of atomic positions M4 into (0.25, 0, 0), M5 into (0.375, 0.375, 0.375) and M6 into (0.125, 0.125, 0.125) reveals an ordered idealized structure with a void (?) in the 8c site (1/4,1/4,1/4) as shown in Fig. 2b. An important implication of such an idealized structure is that all atoms M1, M2, M3 and M4 have the same cubic coordination formed by 8 aluminum atoms, whereas two aluminum atoms M5 and M6 are surrounded by different cubes [Ti_3Ni_3Al?] and [Ti_3Ni_3Ni?]. From this point of view one can assume that the coordination polyhedra in the real structure of the $Ti_6Al_7Ni_{17}$ are similar to that in body-centered W: a cube in the first coordination sphere and an octahedron in the second sphere. In fact, we must take into account the distortions of the cubic environment due to the difference in atomic radii and the above-mentioned hole in 8c. Therefore in the real structure of $Ti_6Al_7Ni_{17}$ the coordination of M1 atoms is a regular cube in the first coordination sphere, and an octahedron in the second sphere, whilst the next nearest neighbor coordination for M2 atoms is an octahedron but a cube for the second neighbor shell. Atoms M3 and M4 are surrounded by distorted tetragonal prisms, which are formed by eight aluminum atoms M5 and M6, but coordination polyhedra of M4 also include one additional aluminum atom M2 (distorted tetragonal prism with CN = 9). Coordination of the M5 and M6 atoms are more complicated, but still reveal their original cube-octahedral nature (Fig. 2a).

The crystal structure presented on Fig. 2a, and interatomic distances in Table 1 reveal a rather short distance Al2–Ti4 (about 0.250 nm) in comparison with the atomic radii of the elements ($r_{Al} = 0.1432$ nm, $r_{Ti} = 0.1448$ nm and $r_{Ni} = 0.1246$ nm), which is more compatible with distances Al–Ni or Ti–Ni than with Al–Ti bonds. Taking this into account one can also conceive a model where Ni1 and Al2 atom sites are interchanged. However, such possibility was ruled out by both neutron and X-ray single crystal intensity data. A relatively large reduction of the bond lengths Al–Al (about 0.270 nm) and Al–M (0.243–0.248 nm) is observed. An interesting aspect is the absence of bonding between titanium and elements of the 8-group; we therefore may assume a rather strong hybridization of Ti–Al and Al–Ni bonds in G-phases resulting in a significant decrease of their bond-lengths. Such behavior is also true for binary phases, $TiAl_2$ and AlM {M = Fe,Co,Ni}, where we encounter bond lengths of

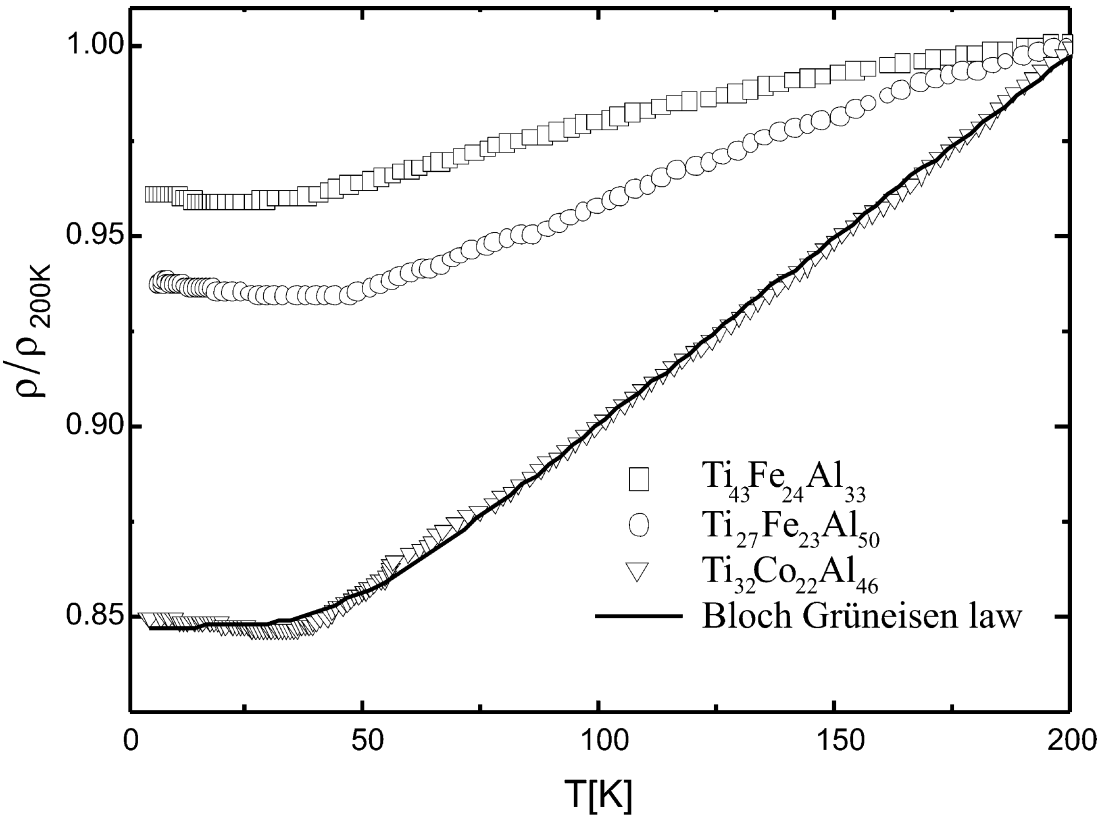

Fig. 3. Normalized resistivity $\rho(T)/\rho_{200\ K}$ for $Ti_{27}Fe_{23}Al_{50}$, $Ti_{43}Fe_{24}Al_{33}$ and $Ti_{32}Co_{22}Al_{46}$.

about 0.267 nm for Al–Al and Al–Ti but values of 0.247–0.249 nm for Al–M in AlM compounds. It is furthermore interesting to note, that M1-atoms in $Ti_6M_7Al_{17}$ and M-atoms in AlM (CsCl structure) have identical cubic coordination and, therefore have corresponding interatomic distances, which are about 10% shorter in comparison with the sum of atomic radii. Interatomic distances are close for all G-phases from the Ti–M–Al {M = Fe–Co–Ni} systems regardless the difference in composition. This merely explains from the rather similar atomic radii of Fe, Co and Ni, and from practically constant contents (23–24 at.%) of these metals in the G-phases. No significant distortion of the parent lattice of the G-phase due to a splitting of the 24e sites in $Ti_6Ni_7Al_{17}$ (annealed at 900 °C) was observed (compare corresponding data in Tables 1 and 3).

3.5. Resistivity and hydrogen absorption of G-phases

The temperature dependent electrical resistivity $\rho(T)/\rho(200\ K)$ of $Ti_{27}Fe_{23}Al_{50}$, $Ti_{43}Fe_{24}Al_{33}$ and $Ti_{32}Co_{22}Al_{46}$ is shown in Fig. 3. All compounds are characterized by relatively large values of the electrical resistivity with metal-like behavior. The residual resistivities for $Ti_{27}Fe_{23}Al_{60}$, $Ti_{43}Fe_{24}Al_{33}$ and $Ti_{32}Co_{22}Al_{46}$ are 0.85, 1.73 and 0.97 mΩ cm, respectively. Resistivity data of $Ti_{32}Co_{22}Al_{46}$, as shown in Fig. 3, were accounted for in terms of the Bloch–Grüneisen formula

$$\rho(T) = \rho_0 + 4R\Theta_D\left(\frac{T}{\Theta_D}\right)^5 \int_0^{\Theta_D/T} \frac{x^5 dx}{(e^x - 1)(1 - e^{-x})} \qquad (1)$$

with ρ_0 the residual resistivity, Θ_D the Debye temperature and R a temperature independent electron-phonon interaction constant. Least squares fits of Eq. (1) to the experimental data reveal a Debye temperature typical for soft intermetallic compounds ($\Theta_D \approx 300$ K).

Hydrogen absorption was studied for the following compounds: $Ti_{23}Fe_{26}Al_{51}$, $Ti_{44}Fe_{26}Al_{30}$, $Ti_{30}Co_{25}Al_{45}$, $Ti_{47}Co_{28}Al_{25}$ and $Ti_{23}Ni_{24}Al_{53}$. In the case of the Ti-poor compounds up to 44 at.% Ti no measurable amount of absorbed hydrogen could be detected, even after loading times of several weeks. Only for the compound, $Ti_{47}Co_{28}Al_{25}$, 8.57 mg hydrogen was absorbed, corresponding to 0.8 wt.%.

4. Conclusion

The crystal structure of G-phases in ternary systems Ti–M–Al {M = Fe,Co,Ni} was established by means of X-ray single crystal and neutron powder diffraction and reveals a new filled variant of the $Mg_6Cu_{16}Si_7$-type structure ($Ti_6Al_7M_{17}$), which is closely related to the structures of Th_6Mn_{23}, $Sc_{22}Ir_8$ and $Zr_6Zn_{23}Si$. Although there is no doubt about the filling or partial filling of the 4b site by metal atoms, crystal chemistry of these

G-phases seems to be more complicated with respect to deformation of coordination figures due to a split of the 24e position, which was observed in $Ti_6Al_7Ni_{17}$ annealed at 900 °C. The stoichiometry of $Ti_6Al_7M_{17}$ is to be considered as ideal composition within or close to the ternary homogeneity region of the G-phases formed by Fe and Ni at 900 °C, whilst it is outside the cobalt based phase solution which shows a higher degree of statistical distribution of Al and Ti atoms in the crystal structure. Crystal structures of the related G-phases in the Hf–Ni–Al and Ti–Si–Ni systems were inspected by Rietveld refinement of the X-ray powder intensity data. While $Hf_6Al_{16}Ni_7$ was found to crystallize with $Mg_6Cu_{16}Si_7$-type, $Ti_6Ni_{16}Si_8$ reveals a filled variant of the $Mg_6Cu_{16}Si_7$ structure.

The absence of any absorbed hydrogen in the Ti–M–Al G phases (M = Fe,Co,Ni) for compositions with less than 44 at.% Ti, is of particular interest in view of a perspective use of G-phases as creep resistance enhancing precipitates (age hardening) in TiAl-based duplex alloys.

Acknowledgements

The research reported herein was sponsored by the Austrian National Science Foundation FWF under grant PP14761.

References

[1] Huneau B, Rogl P, Zeng K, Schmid-Fetzer R, Bohn M, Bauer J. Intermetallics 1999;7:1337.
[2] Zeng K, Schmid-Fetzer R, Huneau B, Rogl P, Bauer J. Intermetallics 1999;7:1347.
[3] Ding JJ, Rogl P, Chevalier B, Etourneau J. Intermetallics 2000; 8:1377.
[4] Ding JJ, Rogl P, Schmidt H, Podloucky R, Visn Lvivsk UN-TU. Ser Khim 2000;39C:136.
[5] Ganglberger E, Nowotny N, Benesovsky F. Monatshefte für Chemie 1966;97:829.
[6] Villars P, Calvert LD. Pearson's handbook of crystallographic data for intermetallic phases. 2nd ed. OH: ASM-International; 1991.
[7] Parthé E, Gelato L, Chabot B, Penzo M, Cenzual K, Gladyshevskii R. TYPIX standardized data and crystal chemical characterization of inorganic structure types. Berlin, Heidelberg: Springer-Verlag; 1994.
[8] Markiv VY, Storoshenko AI. Dopov Akad Nauk Ukr RSR, Ser A 1973;35:941.
[9] Chabot B, Cenzual K, Parthe E. Acta Crystallogr 1980;36B:7.
[10] Chen X, Jeitschko W, Gerdes MH. J Alloys Compounds 1996; 234:12.
[11] Hardman K, Rhyne JJ, Smith K, Wallace WE. J Less Common Metals 1980;74:97.
[12] Jacob I. Solid State Commun 1981;40(11):1015.
[13] Bergman G, Waugh JLT. Acta Crystallogr 1956;9A:214.
[14] Rodriguez-Carvajal J. FULLPROF: a program for rietveld refinement and pattern matching analysis. Physica B 1993;192:55.
[15] Nonius Kappa CCD program package COLLECT, DENZO, SCALEPACK, SORTAV. The Netherlands: Nonius Delft; 1998.
[16] Sheldrick GM. SHELX-97, program for crystal structure refinement. University of Göttingen, Germany [Windows version by McArdle, Natl. Univ. Ireland, Galway]; 1997.
[17] Ganglberger E, Nowotny N, Benesovsky F. Monatshefte für Chemie 1966;97:219.
[18] Palm M, Inden G, Thomas N. J Phase Equilibria 1995;16(3):209.
[19] Palm M, Gorzel A, Letzig D, Sauthoff G. In: Nathal MV et al., editors. Structural intermetallics. The Minerals, Metals & Materials Society; 1997. p. 885.
[20] Gorzel A, Palm M, Sauthoff G. Z Metallkd 1999;90:64.
[21] Raghavan V. J Phase Equilibria 2002;23(4):367.
[22] Levin L, Tokar A, Talianker M, Evangelista E. Intermetallics 1999;7:1317.
[23] Gladishevskii EI, Kripyakevich PI, Kuz'ma YuB, Teslyuk MYu. Krystallographiya 1961;6:615.
[24] Spiegel FX, Bardos D, Back PA. Trans Met Soc AIME 1963; 227:575.
[25] Hu X, Chen G, Ion C, Ni K. J Phase Equilibria 1999;20(5):508.
[26] Florio JV, Rundle RE, Snow AI. Acta Crystallogr 1952;5A:449.